First-principles dynamics treatment of light emission in collisions between alkali-metal atoms and noble-gas atoms at 10 keV

Alexander B. Pacheco, Andrés Reyes,* and David A. Micha
Quantum Theory Project, Departments of Chemistry and Physics, University of Florida, Gainesville, Florida 32611-8435, USA
(Received 7 September 2006; published 20 December 2006; publisher error corrected 22 December 2006)

Collision-induced light emission during the interaction of an alkali-metal atom and a noble-gas atom is treated within a first-principles, or direct, dynamics approach that calculates a time-dependent electric dipole for the whole system, and spectral emission cross sections from its Fourier transform. These cross sections are very sensitive to excited diatomic potentials and a source of information on their shape. The coupling between electronic transitions and nuclear motions is treated with atomic pseudopotentials and an electronic density matrix coupled to trajectories for the nuclei. A recently implemented pseudopotential parametrization scheme is used here for the ground and excited states of the LiHe system, and to calculate state-to-state dipole moments. To verify the accuracy of our new parameters, we recalculate the integral cross sections for the LiHe system in the keV energy regime and obtain agreement with other results from theory and experiment. We further present results for the emission spectrum from 10 keV Li$(2s)$+He collisions, and compare them to experimental values available in the region of light emitted at 300–900 nm.

DOI: 10.1103/PhysRevA.74.062714 PACS number(s): 34.50.−s

I. INTRODUCTION

Light emission during the collisions of two atoms can be described in terms of stationary wave functions for the initial and final quantum states of the diatomic system. Spectral intensities of emission follow then from the state-to-state transition integrals of the dipole operator for the atomic pair. General aspects of light emission were covered in an early review [1] along these lines. Work was published later on using diatomic stationary states obtained from diatomic potentials, their couplings, and dipole integrals, and was also reviewed [2,3]. The present contribution is based on an alternative approach, where the dynamics of the system of electrons and nuclei are directly treated starting from the interaction of all charges, and accounting for the coupling of electronic transitions and nuclear motions within a first-principles, or direct, description of the dynamics that does not require a preliminary calculation of diatomic potentials and couplings. This was developed using electronic density matrices coupled to equations of motion derived in an eikonal (or short-wavelength) time-dependent Hartree-Fock approximation, and called the Eik-TDHF approach [4,5]. This method has been used to describe electronic energy and charge transfer in several applications to one-electron systems [4–7], many-electron systems [8], and pseudo-one-electron systems using l-dependent pseudopotentials [9,10]. Our treatment involves propagation of the full electronic density matrix, which can generate properties of interest during collision such as population, polarization and alignment parameters, electronic and spin angular momentum, and total electronic dipoles.

A collision between atomic species is accompanied by electronic rearrangements as electrons jump between the collisional partners. This rearrangement creates a time-dependent electric dipole that oscillates over time and in accordance with classical electromagnetism, emits light. Spectral light emission and absorption cross sections can then be obtained from the flux of light. Previously, we have used this treatment to study light emission in slow ion-atom collisions, and in particular for the H^++H collision [7] wherein we evolved the system in time by propagating the density matrix to generate a time-dependent dipole that oscillates when the electron jumps between protons.

Our present application of the theory deals with the time evolution of the dipole for the electronic transitions between the ground state (nlm_l) and the excited state $(n'l'm_l')$ of the alkali-metal atom A by collision with a noble-gas atom Ng, in

$$A(nl) + \mathrm{Ng} \rightarrow A(n'l') + \mathrm{Ng} + \mathrm{light}$$

and, in particular

$$\mathrm{Li}(nl) + \mathrm{He} \rightarrow \mathrm{Li}(n'l') + \mathrm{He} + \mathrm{light}.$$

In recent work [11] (referred to as paper I), we discussed the first-principles dynamics of light absorption and emission of alkali-metal and noble-gas excimers, and in particular of the diatomic LiHe, the smallest of these excimers. This was done calculating the optical spectra by reducing the system to a three-body system: a valence electron and the core of Li and a polarizable core of He, using l-dependent atomic pseudopotentials [12]. However, the pseudopotentials commonly used [9,10,12,13], which give excellent results for integral cross sections and light polarization at high energies, do not provide correct positions of molecular transition lines, as found by comparison with experimentally measured or theoretically calculated optical spectra for this system at thermal energies [11,12,14,15]. The reason is that these pseudopotentials give too large a barrier in the $3D\Sigma$ diatomic potential at separations about 8 a.u. between the Li and He atom, as found when compared to an accurate *ab initio* potential.

*Present address: Department of Chemistry, National University of Colombia, Bogota, Colombia.

It has been suggested [12] that the barrier could be lowered by including f orbitals in the basis used to describe the Li atom. Instead, we proposed and implemented using a larger basis set containing both Li and He centered atomic functions, in addition to polarizable core to describe the He atom. We have found that using a basis set on He indeed lowered the barrier in the $3D\Sigma$ potential. We also modified the pseudopotential parameters such that the $3D\Sigma$ potential would be lowered even further, but in such a way that the potentials of the ground and lower excited states of Li were not significantly affected. Using this new parameter set (parameter set B in paper I), we first predicted positions of the molecular transition lines and then proceeded to calculate the absorption spectra for LiHe around 720 K, and obtained good agreement with experimental and other theoretical spectra.

Although calculations at thermal energies compared well with experiments and other theory, we need to verify that the addition of a basis set on He and the new pseudopotential parameter set does not alter the good agreement we previously found for integral cross sections in the keV energy regime [9]. Therefore, in the present work we also calculate the integral cross section for the excitation from the ground state of Li in collisions with He at energies greater than 0.01 eV. Relating to collision-induced light emission, we next present a brief description of our theoretical treatment, followed by state-to-state dipole moments for the LiHe system and the emission spectra for 10 keV $Li(2s)+He$ collisions. For the latter, with the same procedure as in paper I, we calculate the dipole moment during collisions starting from the ground state of the Li and He atoms. We obtain spectral emission cross sections for light emitted with polarization parallel and perpendicular to the direction of an incoming Li, from the second time derivative of the dipole and its Fourier transform. And we finally compare our results to those of Ref. [16] for which the total intensity, I, was proportional to $I_{\parallel}+2I_{\perp}$.

II. THEORETICAL APPROACH

The eikonal–time-dependent molecular orbital (Eik-TDMO) method is a special case of the eikonal–time-dependent Hartree-Fock (Eik-TDHF) method, suitable for systems with one active electron. The implementation of Eik-TDHF and Eik-TDMO methods has been described in great detail in previous articles [4–10]. In paper I, we have presented the Eik-TDMO method including atomic pseudopotentials to calculate the time-dependent dipole moment; we summarize here the relevant equations for the calculations that follow.

A. The eikonal–time-dependent molecular orbital method including atomic pseudopotentials

We begin by writing the Hamiltonian for classical motions as

$$\mathcal{H} = \frac{\mathbf{P}\cdot\mathbf{P}}{2M} + \mathcal{V}, \tag{1}$$

where $\mathbf{P}$ is the relative momentum of the nuclei and M is the reduced mass of the system. The effective potential, $\mathcal{V}$, is given by

$$\mathcal{V} = \frac{\mathrm{Tr}(\hat{\rho}\hat{H}_{\mathrm{el}})}{\mathrm{Tr}(\hat{\rho})}, \tag{2}$$

where $\hat{\rho}=|\psi\rangle\langle\psi|$ is the electronic density operator and $\hat{H}_{\mathrm{el}}$ is the electronic Hamiltonian including l-dependent atomic pseudopotentials given by

$$\hat{H}_{\mathrm{el}} = -\frac{1}{2}\nabla_{r_A}^2 + V_A(\mathbf{r}_A) + V_B(\mathbf{r}_B) + V_{\mathrm{ec}}(\mathbf{r}_A,\mathbf{R}) + V_{\mathrm{cc}}(R). \tag{3}$$

Here A refers to the alkali-metal atom and B refers to the noble-gas atom; $\mathbf{r}_\mu$ is the position vector of the valence electron of the alkali-metal atom from the core μ and $\mathbf{R}$ is the position vector of B with respect to A such that $\mathbf{r}_B=\mathbf{r}_A-\mathbf{R}$.

The term $V_\mu(\mathbf{r}_\mu)$ describes the interaction between the valence electron of the alkali-metal atom and the core μ and is given by

$$V_\mu(\mathbf{r}_\mu) = \frac{Q_\mu}{r_\mu} + \sum_{l,i} B_{l,i}\exp(-\beta_{l,i}r_\mu^2)P_{l,\mu} + V_\mu^{\mathrm{pol}}(\mathbf{r}_\mu), \tag{4}$$

where Q_μ is the net charge of the core μ seen by the e^- at an infinite distance, $B_{l,i}$ and $\beta_{l,i}$ are pseudopotential parameters adjusted to experimental data, and $P_{l,\mu}$ is the projection operator on angular symmetry l. The first two terms in the above equation describe the Coulomb and the l-dependent pseudopotential, respectively. The third term describes the interaction of the electron with the polarizable core and is given as (for each core A and B)

$$V_A^{\mathrm{pol}}(\mathbf{r}_A) = -\frac{\alpha_A^d}{2r_A^4}w(r_A,\delta)^2, \tag{5}$$

$$V_B^{\mathrm{pol}}(\mathbf{r}_B) = -\frac{\alpha_B^d}{2r_B^4}w(r_B,\delta)^4 - \frac{\alpha_B^{q\prime}}{2r_B^6}w(r_B,\delta)^6, \tag{6}$$

where α_μ^d is the dipole polarizability of the core μ and $w(r,\delta)=1-\exp(-\delta r^2)$ stands for a cutoff function with an adjustable parameter δ. The parameter $\alpha_B^{q'}$ is defined as $\alpha_B^{q'}=\alpha_B^q-6\beta_1$, where β_1 is the dynamical correction to the static quadrupole polarizability, α_B^q, of the noble-gas atom.

The term V_{ec} is the so-called cross term, which arises from the polarization of B by both e^- and A, and is given by

$$V_{\mathrm{ec}}(\mathbf{r}_A,\mathbf{R}) = Q_A\alpha_B^d\frac{P_1(\cos\theta)}{R^2r_B^2}w^2(r_B,\delta) + Q_A\alpha_B^q\frac{P_2(\cos\theta)}{R^3r_B^3}w^3(r_B,\delta), \tag{7}$$

where P_1 and P_2 are the Legendre polynomials and θ is the angle between the vectors $-\mathbf{R}$ and $\mathbf{r}_B$.

The core-core interaction is assumed to have the form [17]

$$V_{\mathrm{cc}}(R) = a\exp(-bR) - \frac{1}{2}\frac{\alpha_B^d}{(R^2+d_B^2)^2} - \frac{1}{2}\frac{\alpha_B^{q''}}{(R^2+d_B^2)^3}, \tag{8}$$

where $\alpha_B^{q''}=\alpha_B^q+2\alpha_B^d d_B^2$.

We expand the time-dependent molecular orbitals ψ in terms of linear combinations of traveling atomic functions (TAFs) $\{\xi\}$ with expansion coefficients c and write the density operator in the basis of TAFs as

$$\hat{\rho}(t) = \sum_{pq} |\xi_p\rangle \Gamma_{pq}^{(i)}(t) \langle \xi_q| = |\boldsymbol{\xi}\rangle \boldsymbol{\Gamma}^{(i)} \langle \boldsymbol{\xi}|, \tag{9}$$

where $\Gamma_{pq}^{(i)} = \Sigma_{\text{occ } i} c_{pi}^*(t) c_{qi}(t)$ are the density matrix elements starting in state i. The differential equation for the density operator,

$$\hat{H}_{\text{el}}\hat{\rho} - \hat{\rho}\hat{H}_{\text{el}} = i\hbar \partial\hat{\rho}/\partial t, \tag{10}$$

is written in the basis of TAFs to obtain a differential equation for the density matrix as

$$i\dot{\boldsymbol{\Gamma}} = \mathbf{W}\boldsymbol{\Gamma} - \boldsymbol{\Gamma}\mathbf{W}^\dagger, \tag{11}$$

$$\mathbf{W} = \mathbf{S}^{-1}\mathbf{H}_T, \tag{12}$$

where $\mathbf{S} = \langle \boldsymbol{\xi} | \boldsymbol{\xi} \rangle$ is the overlap matrix and $\mathbf{H}_T$ is the Hamiltonian matrix. The propagation of the density matrix is carried out using the *relax-and-drive* procedure [4]. The dynamics of the system is carried out by coupling the above differential equation for the density matrix with the Hamilton's equations for the classical motion of the nuclei,

$$d\mathbf{R}/dt = \partial\mathcal{H}/\partial\mathbf{P}, \quad d\mathbf{P}/dt = -\partial\mathcal{H}/\partial\mathbf{R}. \tag{13}$$

B. Evaluation of the electric dipole

The total dipole moment $\mathbf{D}$ is given as the sum of the electronic dipole $\mathbf{D}_{\text{el}}$ and the induced dipole moment $\mathbf{D}_{\text{in}}$ as

$$\hat{\mathbf{D}} = \hat{\mathbf{D}}_{\text{el}} + \hat{\mathbf{D}}_{\text{in}} \tag{14}$$

$$= -\hat{\mathbf{r}}_A + \sum_\lambda \left(\frac{\hat{\mathbf{r}}_\lambda}{r_\lambda^3}[1 - \exp(-r_\lambda^2 \delta_\lambda)] - Q_{\mu\neq\lambda}\frac{\hat{\mathbf{R}}}{R^3} \right), \tag{15}$$

where $\mathbf{r}_\lambda$ is the position vector of the electron from core λ, $\mathbf{R}$ is the position vector of the noble gas with respect to the alkali-metal atom, and Q_λ is the charge of core λ. The transition dipole moment (TDM) between molecular states m and n is given by

$$\mathbf{D}_{mn} = \langle \Psi_m | \hat{\mathbf{D}} | \Psi_n \rangle, \tag{16}$$

where $\hat{\mathbf{D}} = \mathbf{n}_x\hat{D}_x + \mathbf{n}_y\hat{D}_y + \mathbf{n}_z\hat{D}_z$, $\mathbf{n}_i$ is a unit vector along the ith axes, and

$$|\langle \Psi_m | \hat{D} | \Psi_n \rangle|^2 = |\langle \Psi_m | \hat{D}_x | \Psi_n \rangle|^2 + |\langle \Psi_m | \hat{D}_y | \Psi_n \rangle|^2 + |\langle \Psi_m | \hat{D}_z | \Psi_n \rangle|^2. \tag{17}$$

If the two states are identical, i.e., $m=n$, then we obtain the dipole moment of the state n.

The average dipole is given as the expectation value of the dipole operator, and in a basis of TAFs is given in terms of the density matrix for initial state i as

$$\mathbf{D}^{(i)} = \text{Tr}[\boldsymbol{\Gamma}^{(i)} \langle \boldsymbol{\xi} | \hat{\mathbf{D}} | \boldsymbol{\xi} \rangle]. \tag{18}$$

C. Time and frequency domain spectra

The electric $\mathbf{E}$ and magnetic $\mathbf{B}$ fields for the light emitted by the dipole [7,18] are given in SI units as

$$\mathbf{E}(\mathbf{r}_{\text{LD}}, t) = \frac{\mu_o}{4\pi r_{\text{LD}}}\{[\mathbf{n}_r \cdot \ddot{\mathbf{D}}(t_r)]\mathbf{n}_r - \ddot{\mathbf{D}}(t_r)\}, \tag{19}$$

$$\mathbf{B}(\mathbf{r}_{\text{LD}}, t) = -\frac{\mu_o}{4\pi r_{\text{LD}} c}[\mathbf{n}_r \times \ddot{\mathbf{D}}(t_r)], \tag{20}$$

where μ_o is the permeability of free space, c is the speed of light, $\mathbf{r}_{\text{LD}}$ is the location of the light detector, $t_r = t - r_{\text{LD}}/c$, and $\mathbf{n}_r = \mathbf{r}_{\text{LD}}/r_{\text{LD}}$.

In the classical treatment, the power P_k radiated per unit solid angle for a single impact parameter b in terms of the Poynting vector, $\mathbf{S}(\mathbf{r}_{\text{LD}}, t) = (1/\mu_o)(\mathbf{E} \times \mathbf{B})$ for each component $k = \perp, \parallel$ to the direction of initial motion of the projectile, is given by

$$\left(\frac{dP_k}{d\Omega_{\text{LD}}}\right)_{b,\Phi} = \left(\frac{d^2E_k}{dt d\Omega_{\text{LD}}}\right)_{b,\Phi} = \mathbf{S}_k \cdot \mathbf{n}_{\text{LD}} r_{\text{LD}}^2 = |A_k(t;b,\Phi)|^2, \tag{21}$$

where the impact parameter $b = b(\Theta)$, and

$$A_k(t;b,\Phi) = \sqrt{\frac{\mu_o}{16\pi^2 c}}\ddot{D}_k(t;b)\sin[\Theta'_{\text{LD}}(t;b,\Phi)] \tag{22}$$

$$= \sqrt{\frac{\mu_o}{16\pi^2 c}}\ddot{D}_{k,T}(t;b,\Phi) \tag{23}$$

is a constant times the component of the dipole second derivative projected on a plane perpendicular (or transversal) to the detector's direction.

We carry out intensity and cross-section calculations in the frequency domain using the Fourier transform of $A_k(t;b,\Phi)$,

$$\tilde{A}_k(\omega) = \frac{1}{\sqrt{2\pi}}\int_{-\infty}^{\infty} A_k(t) e^{i\omega t} dt \tag{24}$$

satisfying $\tilde{A}_k(\omega)^* = \tilde{A}_k(-\omega)$ insofar $A_k(t)$ is real.

Integrating over frequency, the total energy per unit solid angle computed in the frequency domain is then

$$\left(\frac{dE_k}{d\Omega_{\text{LD}}}\right)_{b,\Phi} = 2\int_0^\infty |\tilde{A}_k(\omega;b,\Phi)|^2 d\omega \tag{25}$$

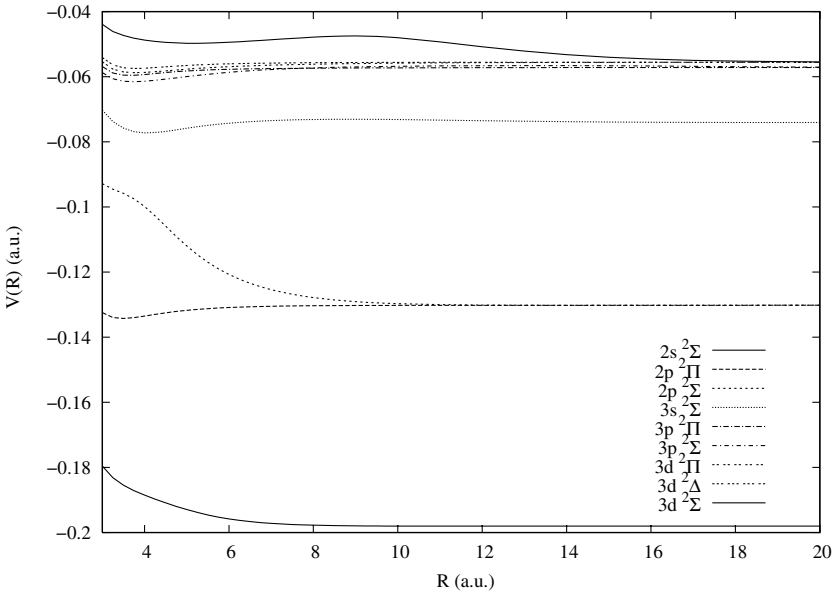

FIG. 1. Potential-energy curves $V(R)$ for LiHe using basis set IIB (from Table I of Ref. [11]) vs the interatomic distance R.

$$= \frac{2\mu_o}{16\pi^2 c}\int_0^\infty |\ddot{\tilde{D}}_{k,T}(\omega;b,\Phi)|^2 d\omega \tag{26}$$

from which we can calculate the intensity of light emitted for each impact parameter per unit solid angle and unit frequency as

$$\left(\frac{dI_k}{d\Omega_{\rm LD}}\right)_{b,\Phi} = \left(\frac{d^2E_k}{d\omega d\Omega_{\rm LD}}\right)_{b,\Phi} = \frac{2\mu_o}{16\pi^2 c}|\ddot{\tilde{D}}_{k,T}(\omega;b,\Phi)|^2. \tag{27}$$

An alternative expression can be obtained in terms of the Fourier transform of the dipole, using

$$\ddot{\tilde{D}}_{k,T}(\omega;b,\Phi) = -\omega^2 \tilde{D}_{k,T}(\omega;b,\Phi), \tag{28}$$

which gives the intensity of light emitted for each impact parameter integrated over all solid angles as [19,20]

$$I_k(\omega;b) = \frac{\mu_o \omega^4}{3\pi c}|\tilde{D}_{k,T}(\omega;b)|^2. \tag{29}$$

The energy emission cross section per unit solid angle in the frequency domain is obtained by integrating the total power over b and Φ,

$$\frac{d^2Q_k}{d\omega d\Omega_{\rm LD}} = \int_0^\infty dbb \int_0^{2\pi} d\Phi \left(\frac{d^2E_k}{d\omega d\Omega_{\rm LD}}\right)_{b,\Phi} \tag{30}$$

$$= \frac{2\mu_o \omega^4}{16\pi^2 c}\int_0^\infty dbb \int_0^{2\pi} d\Phi |\tilde{D}_{k,T}(\omega;b,\Phi)|^2. \tag{31}$$

The total energy emission cross section per unit solid angle and unit frequency, $d^2Q/(d\omega d\Omega_{\rm LD})$, is obtained by adding over the two k components, from which one obtains the total

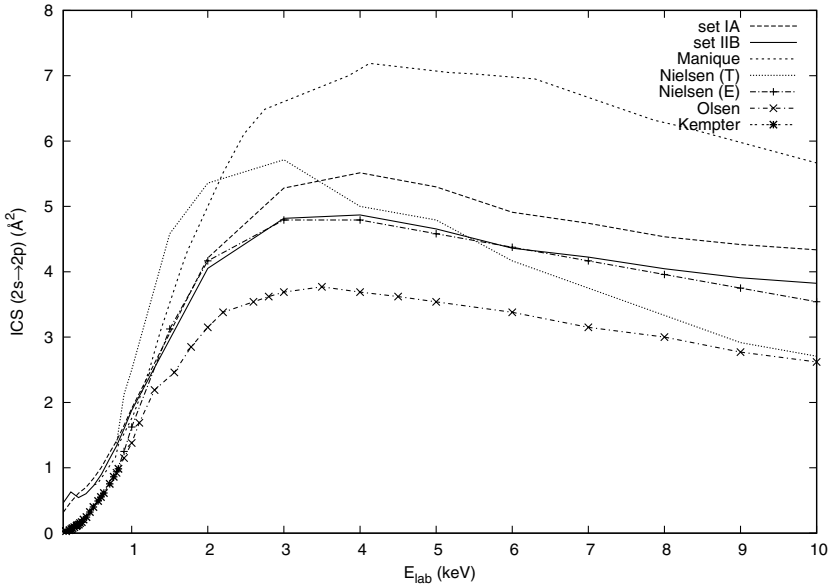

FIG. 2. Integral cross section for Li(2s)+He. Manique: Ref. [21], Nielsen: Ref. [22], Olsen: Ref. [23], Kempter: Ref. [24]. The parentheses for Nielsen's result are for theory (T) and experiment (E).

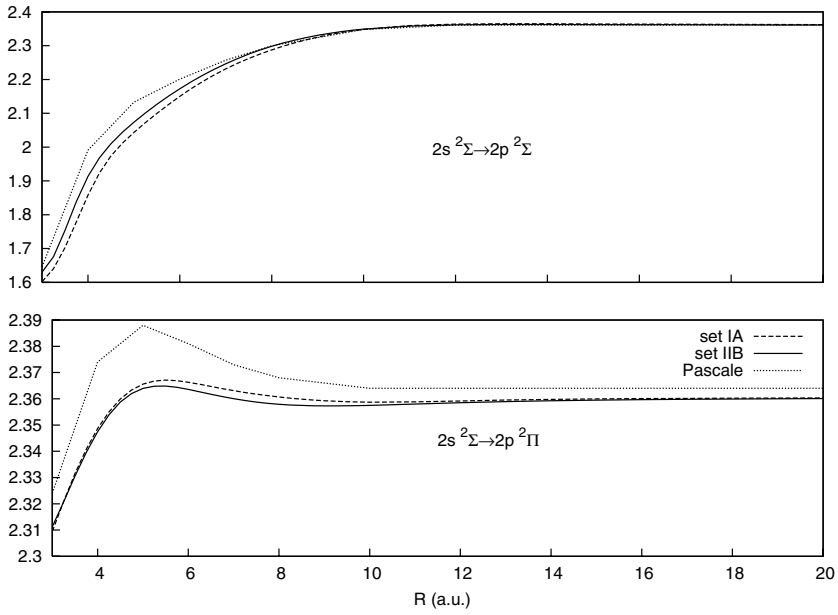

FIG. 3. Transition dipole moment from $2s\ ^2\Sigma \rightarrow 2p(^2\Sigma, ^2\Pi)$. Pascale: Ref. [17].

emission cross section per unit frequency to compare with experimental cross section as

$$\frac{d\sigma_{\mathrm{em}}(\omega)}{d\omega} = \frac{1}{\hbar\omega}\sum_k \frac{dQ_k}{d\omega} \tag{32}$$

$$= \frac{\mu_o \omega^3}{3\pi\hbar c}\int_0^\infty dbb\sum_k |\tilde{D}_{k,T}(\omega;b)|^2. \tag{33}$$

The energy $E_k(b)$ emitted per collision at impact parameter b for each polarization can be obtained by integrating over frequency the intensity of light emitted I_k,

$$E_k = \int I_k d\omega = \int d\omega \frac{\mu_o \omega^4}{3\pi c}|\tilde{D}_{k,T}(\omega;b)|^2. \tag{34}$$

III. RESULTS AND DISCUSSION

A. Integral cross section in the keV energy regime

In paper I, we presented results for the diatomic potential using a basis set of atomic orbitals centered at only the Li atom, and using atomic pseudopotential parameters in the literature, in what we called set IA, and we also presented results for a basis set centered at both Li and the He atom, and a new parametrization scheme for the pseudopotential parameters, called set IIB and shown in Table I of Ref. [11], that gave absorption spectra in good agreement with published spectra [14]. This procedure provided excited-state diatomic potentials with the correct shapes, as shown in Fig. 1. Even though we have already found good agreement using these parameters for spectra at thermal energies, we need to verify that this new proposed scheme gives satisfactory results also at high collision energies, and that they are consis-

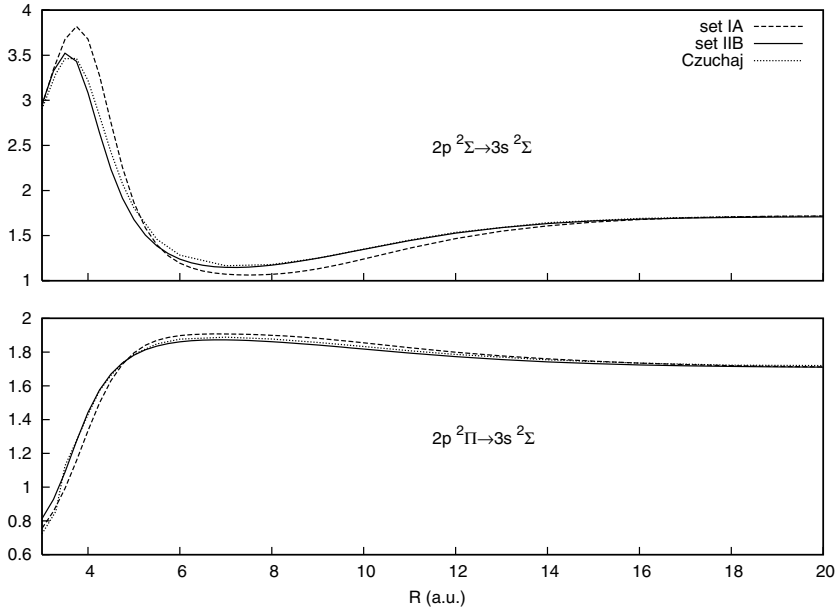

FIG. 4. Transition dipole moment from $2p(^2\Sigma, ^2\Pi) \rightarrow 3s\ ^2\Sigma$. Czuchaj: Ref. [12].

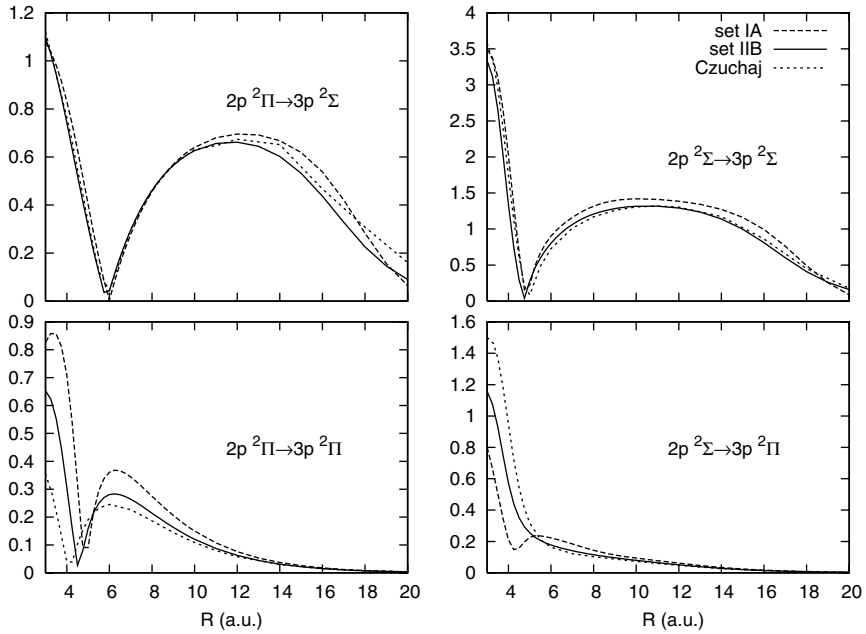

FIG. 5. Transition dipole moment from $2p(^2\Sigma, ^2\Pi) \rightarrow 3p(^2\Sigma, ^2\Pi)$. Czuchaj: Ref. [12].

tent with our previously published work [9]. To achieve this goal, we have recalculated the integral cross section for the Li-He system for energies 0.01 eV $< E_{\text{lab}} <$ 10 keV using sets IA and IIB described in paper I and compared the results with experiments and theory [21–25]. In this section, we are interested in reproducing the results of calculations in Ref. [9], and comparing them with calculations using set IIB.

We reproduce the results of Ref. [9] and new ones in Fig. 2. While comparing with experimental results, they adjusted the experimental ICS at 3 keV (known only in relative values) to match their calculations. In Fig. 2, we plot our calculated ICS directly and do not adjust the experimental ICS. Our results using both basis sets and pseudopotential parameters are in good agreement over the entire energy range compared to experimental [21–25] and other theoretical [22] values.

B. Dipole moments

In paper I, we presented results for the potential-energy curves using sets IA and IIB. Here, we present results for the state dipole moment and transition dipole moments (TDM) using sets IA and IIB. In Figs. 3–6, we report the TDM's we have obtained for the LiHe collisional system using set IA and IIB, and compare them to similar calculations [12,17]. In Table I, we also report the dipole moment for the ground state of the LiHe collisional system and compare it to those available in the literature [26–28].

Our results for the diatomic state dipole moment and for the state-to-state transition dipoles are in reasonable agreement with published results [12,17,26–28]. Results obtained using set IIB are in better agreement with published results than those obtained using set IA.

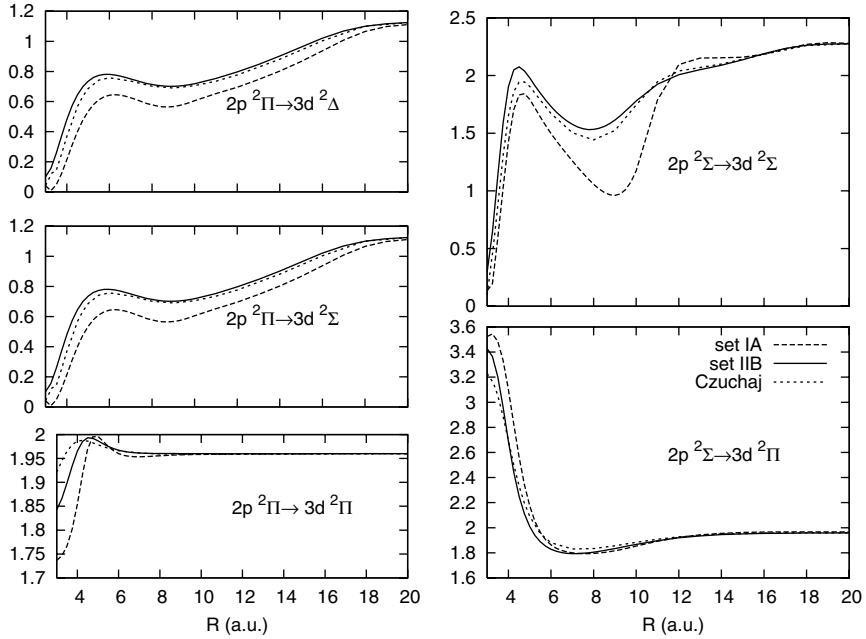

FIG. 6. Transition dipole moment from $2p(^2\Sigma, ^2\Pi) \rightarrow 3d(^2\Sigma, ^2\Pi, ^2\Delta)$. Czuchaj: Ref. [12].

TABLE I. Dipole moment of the $2s^2\Sigma$ state.

				Ref. [27]		
R (a.u.)	Set IA	Set IIB	Ref. [26]	GTO basis	STO basis	Ref. [28]
3.0	1.16492	1.21255	1.372	1.392	1.433	1.339
4.0	0.95069	0.97733	0.992	1.032	1.053	1.003
5.0	0.61668	0.60661		0.615	0.624	0.584
6.0	0.30894	0.30308	0.295	0.316	0.321	0.280
7.0	0.12963	0.12671			0.151	0.118
8.0	0.04314	0.03941	0.059		0.0667	0.0458
10.0	0.01550	0.01495	0.008		0.0113	0.0530

C. Light emission for 10 keV Li($2s$)+He collisions

Having confirmed that the new basis and parameter set gives excellent agreement with experimental and theoretical calculations for ICS in the keV energy regime and good results for the transition dipole moments compared to the pseudopotential calculations of Refs. [12,17], we now present results of calculations for the emission spectra for 10 keV Li($2s$)+He collisions.

Calculations were performed for impact parameters in the range $b=0.0-5.0$ a.u. at intervals of 0.1 a.u., and integrating the equations of motion for electron and nuclei with a constant time interval of $\Delta t=0.1$ a.u. using both basis sets IA and IIB. For the present high-energy collisions, we stopped the calculations at a final distance of 600 a.u. so that the dipole moment had enough uniform oscillations in time to provide detailed spectra using the Fourier transform. The spectra were converged for that final distance of 600 a.u. and a minimum upper limit of 5 a.u. for the impact parameters; further calculations using impact parameters up to 7 a.u. did not change the spectra or the intensity percentages.

In Fig. 7, we plot the intensity as a percentage of the Li($2S-2P$) transition, while in Table II, we compare the intensity percentages of the most prominent Li transition lines with experimental values. We obtain good agreement for all the atomic transition lines except for the Li($3S-2P$) line at large wavelengths, which appears more intense in the measurements. On the other hand, we obtain more intense lines for the molecular transitions $3P(\Sigma,\Pi)$, $3D\Pi\rightarrow 2S\Sigma$, $3P\Sigma\rightarrow 2P\Pi$, $4D\Pi\rightarrow 2P\Sigma$, and $6S\Sigma-3S\Sigma$ at shorter wavelengths, which were not given in Ref. [16]. Intensities calculated using basis II are in better agreement than those using basis I. Also, use of basis functions on He reduces the intensity of the molecular transition by a factor of 1.7 while increasing the intensity of the Li($3S-2P$) by a factor of 1.6. The remaining discrepancies between our calculations and experimental values of intensities might be due to fast internal energy transfer during collisions from higher-energy excited molecular states to the lower-energy state of Li $3S$. This would have as a consequence a decrease of the molecular line intensities and an increase of the atomic line over the observation time.

TABLE II. Comparison of intensities for 10 keV Li($2S$)+He.

λ (nm)	Transition	Ref. [16]	Set IA	Set IIB
323.26	$3P$-$2S$	0.4375	0.72	0.64
460.29	$4D$-$2P$	0.875	1.28	1.04
497.17	$4S$-$2P$	0.375	0.4	0.32
610.36	$3D$-$2P$	10.9375	10.238	10.0
670.78	$2P$-$2S$	100.0	100.0	100.0
812.64	$3S$-$2P$	7.5	0.64	1.04

We have also calculated the energies emitted per collision from Eq. (34) and listed them in Table III for a few impact parameters. Comparison of the emitted electromagnetic energy with the total atomic energy shows that the former is statistically negligible, specifically of the order of 10^{-4} a.u. for the smallest impact parameters compared to a total (kinetic plus binding) atomic energy of the order of 10^2 a.u.

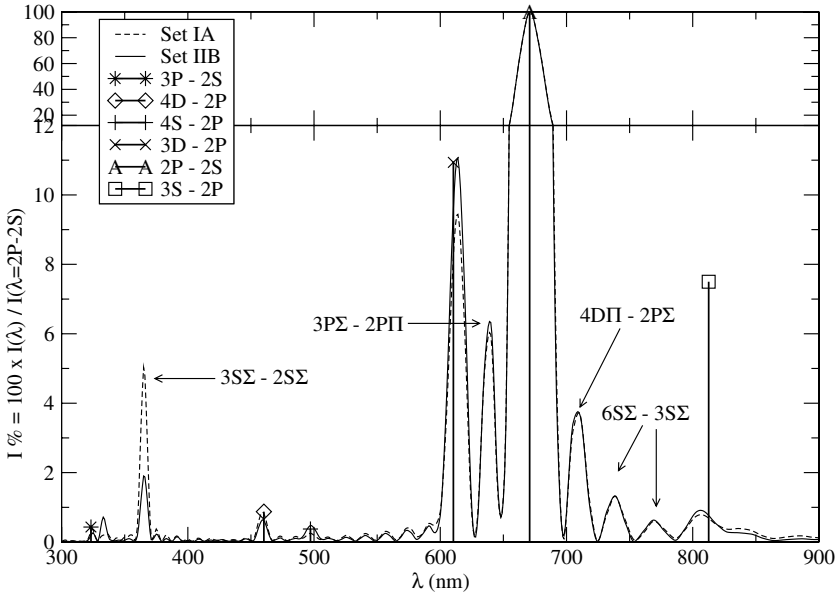

FIG. 7. Emission spectrum for 10 keV Li($2s$)+He.

TABLE III. Energy E_k, for $k=\perp,\parallel$, emitted per collision for 10 keV Li(2*S*)+He for given impact parameter (IP).

	Energy (a.u.)		
IP (a.u.)	$\perp$	$\parallel$	Total
0.50	2.53681×10^{-5}	9.45706×10^{-5}	1.45307×10^{-4}
1.00	1.12594×10^{-7}	5.31064×10^{-7}	7.56253×10^{-7}
1.50	1.07473×10^{-7}	1.23268×10^{-7}	3.38214×10^{-7}
2.00	2.95861×10^{-7}	1.64622×10^{-7}	7.56345×10^{-7}
2.50	1.28569×10^{-7}	4.72850×10^{-8}	3.04423×10^{-7}
3.00	1.81260×10^{-8}	4.90650×10^{-9}	4.11586×10^{-8}
3.50	7.73032×10^{-9}	1.57192×10^{-9}	1.70326×10^{-8}
4.00	3.13983×10^{-9}	5.23031×10^{-10}	6.80268×10^{-9}
4.50	1.37375×10^{-9}	2.01907×10^{-10}	2.94942×10^{-9}
5.00	6.64118×10^{-10}	9.39242×10^{-11}	1.42216×10^{-9}

This shows that the amount of energy emitted during collisions at each impact parameter is negligible compared to the total energy of the colliding pair. Our semiclassical treatment of light emission is therefore justified by near energy conservation in the atomic system.

IV. CONCLUSION

Atomic pseudopotentials are very convenient and accurate for studies of electronic transitions in interactions of an alkali-metal atom with a noble-gas atom. The transient spectra from alkali-metal atoms and noble-gas atoms interactions are very sensitive to the shapes of potential energies for excited states, and these depend on atomic basis sets and pseudopotential parameters. We have found that using a basis set of atomic functions centered at both Li and He, consistent with their pseudopotentials, decreases the barrier in the $3D\Sigma$ potential while not affecting the potentials of the lower excited and ground states. A large enough basis centered only on the alkali-metal atom, and pseudopotentials with a polarizable core, were sufficient to obtain good comparisons with previously published results for integral cross sections. This is also sufficient to obtain intensities and positions of spectral lines for atomic transitions and lower excitation molecular transitions as seen from our current work and calculations at thermal energies. However, for higher excitations, particularly those involving 3D states, use of a basis set on He in addition to *l*-dependent pseudopotentials is necessary. We have followed a computational procedure based on the simultaneous propagation of the electron density matrix and nuclear trajectories to directly obtain spectral intensities and to compare them with simple theoretical predictions as well as experimental values. The comparison with experiment shows agreement on the location of spectral lines, and for the intensities of the most prominent peaks. The remaining discrepancies might be due to the fast transfer of energy from excited molecular states to excited atomic states during collision and before light is emitted.

To our knowledge, these are the first calculations employing pseudopotentials and basis functions on He, although similar calculations have been carried out for Ar in studies involving Na in Ar clusters and matrices [29,30]. The challenge in our approach has been to generate a good enough basis set to accurately calculate the alkali-metal valence electron–noble-gas-atom interactions. This necessitated highly excited $(2s,2p,3s,\ldots)$ orbitals on He to properly describe a transient He^- ion formed during collisions, and a treatment of the dynamics allowing for the coupling of nuclear motions with electronic rearrangement.

ACKNOWLEDGMENT

This work was partly supported by the National Science Foundation.

[1] U. Fano and J. H. Macek, Rev. Mod. Phys. **45**, 553 (1973).
[2] B. Zygelman, A. Dalgarno, M. Kimura, and N. F. Lane, Phys. Rev. A **40**, 2340 (1989).
[3] M. Kimura and N. F. Lane, Adv. At., Mol., Opt. Phys. **26**, 79 (1990).
[4] D. A. Micha and K. Runge, Phys. Rev. A **50**, 322 (1994).
[5] D. A. Micha, J. Phys. Chem. A **103**, 7562 (1999).
[6] K. Runge and D. A. Micha, Phys. Rev. A **53**, 1388 (1996).
[7] H. F. M. DaCosta, D. A. Micha, and K. Runge, J. Chem. Phys. **107**, 9018 (1997).
[8] K. Runge and D. A. Micha, Phys. Rev. A **62**, 022703 (2000).
[9] A. Reyes and D. A. Micha, J. Chem. Phys. **119**, 12308 (2003).
[10] A. Reyes and D. A. Micha, J. Chem. Phys. **119**, 12316 (2003).
[11] A. B. Pacheco, A. Reyes, and D. A. Micha, J. Chem. Phys. **125**, 154313 (2006).
[12] E. Czuchaj, F. Rebentrost, H. Stoll, and H. Preuss, Chem. Phys. **196**, 37 (1995).
[13] E. Czuchaj, F. Rebentrost, H. Stoll, and H. Preuss, Chem. Phys. **136**, 79 (1989).
[14] W. Behmenburg *et al.*, J. Phys. B **29**, 3891 (1996).
[15] A. B. Pacheco and D. A. Micha, presented at the 44th Sanibel Symposium, St. Simons Island, GA (2005) (unpublished).
[16] N. Andersen and S. E. Nielsen, Adv. At. Mol. Phys. **18**, 265 (1982).
[17] J. Pascale, Phys. Rev. A **28**, 632 (1983).
[18] D. J. Griffiths, *Introduction to Electrodynamics* (Prentice Hall, Englewood Cliffs, NJ, 1989).
[19] D. A. Micha, K. Runge, and H. F. M. DaCosta, Chem. Phys. Lett. **256**, 321 (1996).
[20] H. F. M. DaCosta, D. A. Micha, and K. Runge, Int. J. Quantum Chem. **30**, 257 (1996).
[21] J. Manique, S. E. Nielsen, and J. S. Dahler, J. Phys. B **10**, 1703 (1977).
[22] S. E. Nielsen, N. Andersen, T. Andersen, J. O. Olsen, and J. S. Dahler, J. Phys. B **11**, 3187 (1978).
[23] J. O. Olsen, N. Andersen, and T. Andersen, J. Phys. B **10**, 1723 (1977).
[24] B. Staudenmayer and V. Kempter, J. Phys. B **13**, 309 (1980).

[25] E. Speller, B. Staudenmayer, and V. Kempter, Z. Phys. A **291**, 311 (1979).
[26] C. Bottcher, A. Dalgarno, and E. L. Wright, Phys. Rev. A **7**, 1606 (1973).
[27] M. Krauss, P. Maldonado, and A. C. Wahl, J. Chem. Phys. **54**, 4944 (1971).
[28] J. Pascale, J. Chem. Phys. **67**, 204 (1977).
[29] J. Ahokas, T. Kiljunen, J. Eloranta, and H. Kunttu, J. Chem. Phys. **112**, 2420 (2000).
[30] M. Groß and F. Spiegelmann, J. Chem. Phys. **108**, 4148 (1998).